Hindawi
International Journal of Polymer Science
Volume 2022, Article ID 6815187, 13 pages
https://doi.org/10.1155/2022/6815187

Research Article

Design and Synthesis of Conducting Polymer Bio-Based Polyurethane Produced from Palm Kernel Oil

Muhammad Abdurrahman Munir[1], **Khairiah Haji Badri**[2,3], **Lee Yook Heng**[2], **Ahlam Inayatullah**[4], **Hamid Alkhair Badrul**[4], **Emelda Emelda**[1], **Eliza Dwinta**[1], **Nurul Kusumawardani**[1], **Ari Susiana Wulandari**[1], **Veriani Aprilia**[5], **and Rachmad Bagas Yahya Supriyono**[1]

[1]*Department of Pharmacy, Faculty of Health Science, Alma Ata University, Daerah Istimewa Yogyakarta 55183, Indonesia*
[2]*Department of Chemical Sciences, Faculty of Science and Technology, Universiti Kebangsaan Malaysia, Bangi 43600, Malaysia*
[3]*Polymer Research Center, Universiti Kebangsaan Malaysia, Bangi 43600, Malaysia*
[4]*Faculty of Science and Technology, Universiti Sains Islam Malaysia, Nilai 71800, Malaysia*
[5]*Department of Nutrition Science, Alma Ata School of Health Sciences, Alma Ata University, Daerah Istimewa Yogyakarta 55183, Indonesia*

Correspondence should be addressed to Muhammad Abdurrahman Munir; muhammadabdurrahman2220@gmail.com

Received 11 June 2021; Revised 1 October 2021; Accepted 23 March 2022; Published 7 April 2022

Academic Editor: Joanna Rydz

Polyurethane (PU) is a unique polymer that has versatile processing methods and mechanical properties upon the inclusion of selected additives. In this study, a freestanding bio-based polyurethane film the screen-printed electrode (SPE) was prepared by the solution casting technique, using acetone as solvent. It was a one-pot synthesis between major reactants, namely, palm kernel oil-based polyol and 4,4-methylene diisocyanate. The PU has strong adhesion on the SPE surface. The synthesized bio-based polyurethane was characterized using thermogravimetry analysis, differential scanning calorimetry, Fourier-transform infrared spectroscopy (FTIR), surface area analysis by field emission scanning electron microscope, and cyclic voltammetry. Cyclic voltammetry was employed to study electrocatalytic properties of SPE-polyurethane towards oxidation of PU. Remarkably, SPE-PU exhibited improved anodic peak current as compared to SPE itself using the differential pulse voltammetry method. Furthermore, the formation of urethane linkages (-NHC(O) backbone) after polymerization was analyzed using FTIR and confirmed by the absence of peak at 2241 cm^{-1} attributed to the sp-hydridized carbons atoms of C≡C bonds. The glass transition temperature of the polyurethane was detected at 78.1°C.

1. Introduction

Conducting polymers (CPs) are polymers that can release a current [1]. The conductivity of CPs was first observed in polyacetylene, nevertheless owing to its instability, and the invention of various CPs has been studied and reported such as polyaniline (PANI), poly(*o*-toluidine) (PoT), polythiophene (PTH), polyfluorene (PF), and polyurethane (PU). Furthermore, natural CPs have low conductivity and are often semiconductive. Therefore, it is imperative to improve their conductivity for electrochemical sensor purposes [2–4]. The CPs can be produced from many organic materials and they have several advantages, such as having an electrical current, inexpensive materials, massive surface area, and small dimensions, and the production is straightforward. Furthermore, according to these properties, many studies have been reported by researchers to study and report the variety of CPs applications such as sensors, biochemical applications, electrochromic devices, and solar cells [1, 5]. There is scientific documentation on the use of conductive polymers in various studies such as polyaniline [6], polypyrrole [7], and polyurethane [8–11].

Polyurethane productions can be obtained by using several materials as polyols such as petroleum, coal, and crude oils. Nevertheless, these materials have become very rare to find and the price is very expensive at the same time required a sophisticated system to produce it. The reasons such as price and time consuming to produce polyols have been considered by many researchers; furthermore, finding utilizing plants that can be used as alternative polyols should be done immediately [12]. Thus, to avoid the use of petroleum, coal, and crude oils as raw materials for a polyol, vegetable oils become a better choice to produce polyol in order to obtain a biodegradable polymer. Vegetable oils that are generally used for polyurethane synthesis are soybean oil, corn oil, sunflower seed oil, coconut oil, nuts oil, rapeseed, olive oil, and palm oil [12, 13].

It is very straightforward for vegetable oils to react with a specific group to produce a PU such as epoxy, hydroxyl, carboxyl, and acrylate owing to the existence of (-C=C-) in vegetable oils. Thus, it provides appealing profits to vegetable oils compared to petroleum considering the toxicity, price, and harm to the environment [14, 15]. Palm oil becomes the chosen in this study to produce PU owing to it being largely cultivated in South Asia particularly in Malaysia and Indonesia. It has several profits compared to other vegetable oils such as the easiest materials obtained, the lowest cost of all the common vegetable oils, and recognized as the plantation that has a low environmental impact and removing CO_2 from the atmosphere as a net sequester [16, 17].

The application of bio-based polymer has appealed much attention until now. Global environmental activists have forced researchers to discover another material producing polymers [18]. PUs have many advantages that have been used by many researchers, they are not merely versatile materials but also have the durability of metal and the flexibility of rubber. Furthermore, they can be promoted to replace rubber, metals, and plastics in several aspects. Several applications of PUs have been reported and studied such as textiles, automotive, building and construction applications, and biomedical applications [19, 20]. Polyurethanes are also considered to be one of the most useful materials with many profits, such as possessing low conductivity, low density, absorption capability, and dimensional stability. They are a great research subject due to their mechanical, physical, and chemical properties [21–24].

PU structure contains the urethane group that can be formed from the reaction between isocyanate groups (-NCO) and hydroxyl group (-OH). Nevertheless, several groups can be found in PU structure such as urea, esters, ethers, and several aromatic groups. Furthermore, PUs can be produced from different sources as long as they contain specific materials (polyol and methylene diphenyl diisocyanate (MDI)), making them very useful for specific applications. Thus, according to the desired properties, PUs can be divided into several types such as waterborne, flexible, rigid, coating, binding, sealants, adhesives, and elastomers [25].

PUs are lighter than other materials such as metals, gold, and platinum. The hardness of PU also relies on the number of the aromatic rings in the polymer structure [26, 27], majorly contributed by the isocyanate derivatives. PUs have also a conjugate structure where electrons can move in the main chain that causes electricity produced even the current is low. The current of conjugated linear (π) can be elaborated by the gap between the valence band and the conduction band, or called high energy level containing electrons (HOMO) and lowest energy level not containing electrons (LUMO), respectively [28, 29].

In the recent past, several conventional methods have been developed such as capillary electrophoresis, liquid, and gas chromatography coupled with several detectors. Nevertheless, although chromatographic and spectrometric approaches are well developed for qualitative and quantitative analyses of analytes, several limitations emerged such as complicated instrumentation, expensive, tedious sample preparations, and requiring large amounts of expensive solvents that will harm the users and environment [22–24, 30–33]. Therefore, it is imperative to obtain and develop an alternative material that can be used to analyze a specific analyte. Electrochemical methods are extremely promising methods in the determination of an analyte in samples owing to the high selectivities, sensitivities, inexpensive, requirements of small amounts of solvents, and can be operated by people who have no background in analytical chemistry. In addition, sample preparation such as separation and extraction steps are not needed owing to the selectivity of this instrument where no obvious interference on the current response is recorded [34]. Few works have been reported on the electrochemical methods for the determination of analyte using electrodes combined with several electrode modifiers such as carbon nanotube, gold, and graphene [34, 35]. Nevertheless, the materials are expensive and the production is difficult. Thus, an electrochemical approach using inexpensive and easily available materials as electrode modifiers should be developed [36, 37].

Nowadays, screen-printed electrodes (SPEs) modified with conducting polymer have been developed for various electrochemical sensing. SPE becomes the best solution owing to the electrode having several advantages such as frugal manufacture, tiny size, being able to produce on a large scale, and can be applied for on-site detection [38]. Conducting polymers (CPs) become an alternative to modifying the screen-printed electrodes due to several advantages such as their electrical conductivity, able to capture analyte by chemical/physical adsorption, and large surface area. Thus, CPs are very appealing materials from electrochemical perspectives [39]. Such advantages of SPE encourage us to construct a new electrode for electrochemical sensing, and no research reported on the direct electrochemical oxidation of histamine using a screen-printed electrode modified by bio-based polyurethane. Therefore, this research is the first to develop a new electrode using (screen printed polyurethane electrode) SPPE without any conducting materials.

The purpose of this work was to synthesize, characterize, and study the electrobehavior of polyurethane using cyclic voltammetry (CV) and differential pulse voltammetry (DPV) attached to the screen-printed electrode. To the best of our knowledge, this is the first attempt to use a modified

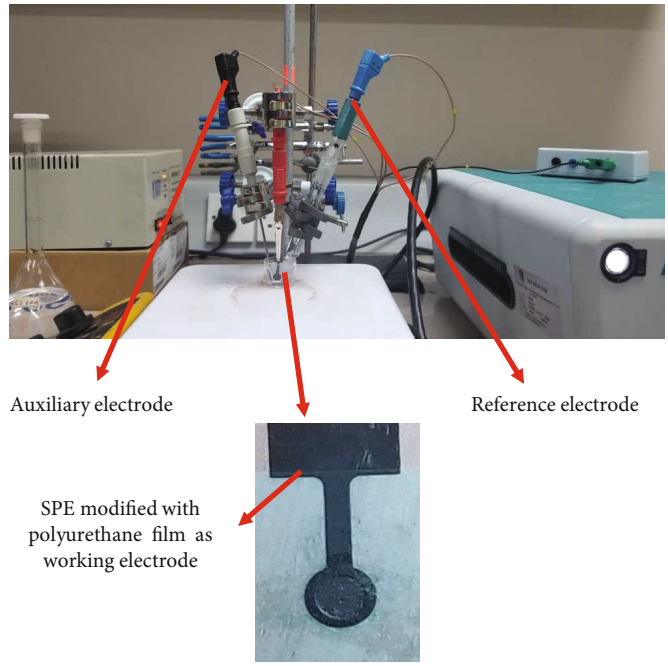

Figure 1: Potentiostat instrument to study the conductivity of SPE modified with polyurethane film using voltammetric approach: CV and DPV.

polyurethane electrode. The electrochemistry of polyurethane mounted onto SPE is discussed in detail. PUs are possible to become an advanced frontier material that has been chemically modified the specific electrodes for bio/chemical sensing application.

2. Experimental

2.1. Chemicals

2.1.1. Synthesis of Bio-Based Polyurethane Film. Palm kernel oil- (PKO-p-) based polyol was supplied by the UKM Technology Sdn Bhd through MPOB/UKM station plant, Pekan Bangi Lama, Selangor, and prepared using Badri et al. [40] method. 4,4-diphenylmethane diisocyanate (MDI) was acquired from Cosmopolyurethane (M) Sdn. Bhd., Klang, Malaysia. Solvents and analytical reagents were benzene (≥99.8%), toluene (≥99.8%), hexane (≥99%), acetone (≥99%), dimethylsulfoxide (DMSO) (≥99.9%), dimethylformamide (DMF) (≥99.8%), tetrahydrofuran (THF) (≥99.8%), and polyethylene glycol (PEG) with a molecular weight of 400 Da obtained from Sigma Aldrich Sdn Bhd, Shah Alam.

2.2. Apparatus. Tensile testing was performed using a universal testing machine model Instron 5566 following ASTM D638 (Standard Test Method for Tensile Properties of Plastics). The tensile properties of the polyurethane film were measured at a velocity of 10 mm/min with a cell load of 5 kN.

The thermal properties were performed using thermogravimetry analysis (TGA) and differential scanning calorimetry (DSC) analysis. TGA was performed using a thermal analyzer of the Perkin Elmer Pyris model with a heating rate of 10°C/min at a temperature range of 30 to 800°C under a nitrogen gas atmosphere. The DSC analysis was performed using a thermal analyzer of the Perkin Elmer Pyris model with a heating rate of 10°C/minute at a temperature range of -100 to 200°C under a nitrogen gas atmosphere. Approximately, 5–10 mg of PU was weighed. The sample was heated from 25 to 150°C for one minute, then cooled immediately from 150 to 100°C for another one minute and finally, reheated to 200°C at a rate of 10°C/min. At this point, the polyurethane encounters changing from elastic properties to brittle due to changes in the movement of the polymer chains. Therefore, the temperature in the middle of the inclined regions is taken as the glass transition temperature (T_g). The melting temperature (T_m) is identified as the maximum endothermic peak by taking the area below the peak as the enthalpy point (ΔH_m).

The morphological analysis of PU film was performed by field emission scanning electron microscope (FESEM) model Gemini SEM microscope model 500-70-22. Before the analysis was carried out, the polyurethane film was coated with a thin layer of gold to increase the conductivity of the film. The coating method was carried out using a sputter-coater. The observations were conducted at a magnification of 200x and 5000x with 10.00 kV (electron high tension (EHT)).

The crosslinking of PU was determined using the soxhlet extraction method. About 0.60 g of PU sample was weighed and put in an extractor tube containing 250 mL of toluene, used as a solvent. This flow of toluene was let running for 24 h. Mass of the PU was weighed before and after the reflux process was carried out. Then, the sample was dried in the conventional oven at 100°C for 24 h in order to get a constant mass. The percentage of crosslinking content known

Table 1: The specification of PKO-p (Badri et al. [40]).

Property	Values
Viscosity at 25°C (cps)	1313.3
Specific gravity (g/mL)	1.114
Moisture content (%)	0.09
pH value	10–11
The hydroxyl number mg KOH/g	450–470

as the gel content can be calculated using Equation (1).

$$\text{Gel content}\,(\%) = \frac{W_o - W}{W} \times 100\%, \quad (1)$$

where W_o is the mass of PU before the reflux process (g) and W is the mass of PU after the reflux process (g).

FTIR spectroscopic analysis was performed using a Perkin-Elmer Spectrum BX instrument using the diamond attenuation total reflectance (DATR) method to confirm the polyurethane, PKO-p, and MDI functional group. FTIR spectroscopic analysis was performed at a wavenumber of 4000 to 600 cm^{-1} to identify the peaks of the major functional groups in the formation of the polymer such as amide group (-NH), urethane carbonyl group (-C=O), isocyanate group (-O=C=N-), and carbamate group (-CN).

2.3. Synthesis of Polyurethane. Firstly, the polyol prepolymer solution was produced by combining palm kernel oil-based polyol and poly(ethylene glycol) (PEG) 400 (100 : 40 g/g), and acetone 30% was used as a solution. The compound was homogenized using a centrifuge (100 rpm) for 5 min. Whereas diisocyanate prepolymer was obtained by mixing 4,4'-diphenylmethane diisocyanate (100 g) to acetone 30%, afterward the mixture was mixed using a centrifuge for 1 min to obtain a homogenized solution. Afterward, diisocyanate solution (10 g) was poured into a container that contains polyol prepolymer solution (10 g) slowly to avoid an exothermic reaction occurring. The mixture was mixed for 30 sec until a homogenized solution was acquired. Lastly, the polyurethane solution was poured on the electrode surface by using the casting method and dried at ambient temperature for 12 h.

2.4. Modification of Electrode. Voltammetric tests were performed using Metrohm Autolab Software (Figure 1) analyzer using cyclic voltammetry method or known as amperometric mode and differential pulse voltammetry. All electrochemical experiments were carried out using screen-printed electrode (diameter 3 mm) modified using polyurethane film as working electrode, platinum wire as the auxiliary electrode, and Ag/AgCl electrode as a reference electrode. All experiments were conducted at a temperature of 20 ± 2°C.

The PU was cast onto the screen-printed electrode (SPE) and analyzed using a single voltammetric cycle between -1200 and +1500 mV (vs Ag/AgCl) of ten cycles at a scanning rate of 100 mV/s in 5 mL of KCl in order to study the activity of SPE and polyurethane film. Approximately, 0.1, 0.3, and 0.5 mg of polyurethane were dropped separately onto the SPE surface, and dried at room temperature. The modified palm-based polyurethane electrodes were then rinsed with deionized water to remove physically adsorbed impurities and residues of unreacted material on the electrode surface. All electrochemical materials and calibration measurements were carried out in a 5 mL glass beaker with a configuration of three electrodes inside it. Platinum wire and silver/silver chloride (Ag/AgCl) electrodes were used as auxiliary and reference electrodes, while a screen-printed electrode that had been modified with polyurethane was applied as a working electrode.

3. Results and Discussion

The synthesis of PU films was carried out using a prepolymerization method which involves the formation of urethane polymer at an early stage. The reaction took place between diisocyanate (MDI) and palm kernel oil-based polyol. Table 1 presents the PKO-p properties used in this study.

The structural chain was extended with the aid of poly(-ethylene glycol) to form flexible and elastic polyurethane film. In order to produce the urethane prepolymer, the isocyanate group (-NCO) attacks with the hydroxyl group (-OH) of polyol (PKO-p) while the other hydroxyl group of the polyol is attacked by the other isocyanate group [41] as shown in Figure 2.

3.1. FTIR Analysis. Figure 3 shows the FTIR spectra for polyurethane, exhibiting the important functional group peaks. According to a study researched by [41], PKO-p reacts with MDI to form urethane prepolymers. The NCO group on MDI reacts with the OH group on polyol whether PKO-p or PEG. It can be seen there are no important peaks of MDI in the FTIR spectra. This is further verified by the absence of an absorption bands at the 2400 cm^{-1} belonging to MDI (-NCO groups). This could also confirm that the -NCO group on MDI had completely reacted with PKO-p to form the urethane -NHC(O) backbone. The presence of amides (-NH), carbonyl urethane group (-C=O), carbamate group (C-NH), and -C-O-C confirmed the formation of urethane chains. In this study, the peak of carbonyl urethane (-C=O) detected at 1727 cm^{-1} indicated that the carbonyl urethane group was bonded without hydrogen owing to the hydrogen reacts with the carbonyl urethane group.

The reaction of polyurethane has been studied by Hamuzan and Badri [42] where the urethane carbonyl group was detected at 1730–1735 cm^{-1} while the MDI carbonyl was detected at 2400 cm^{-1}. The absence of absorption bands at 2250–2270 cm^{-1} associated with N=C=O bond stretching indicates the absence of NCO groups. It shows that the polymerization reaction occurs entirely between NCO groups in MDI with hydroxyl groups on polyols and PEG [43]. The absence of peaks at 1690 cm^{-1} representing urea (C=O) in this study indicated there is no urea formation as a byproduct [44] of the polymerization reaction that possibly occurs due to the excessive water. For the amine (-NH) group, hydrogen bond to -NH and oxygen to form ether, and

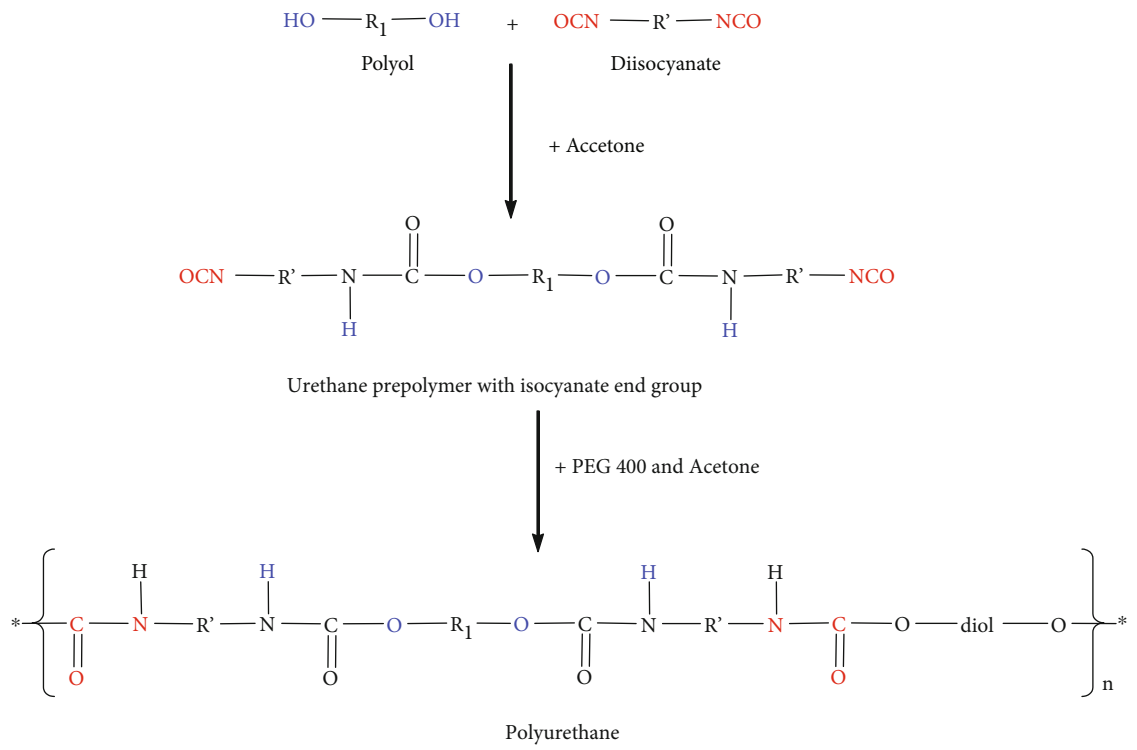

Figure 2: PU production via the prepolymerization method [41].

hydrogen bond to NH and oxygen to form carbonyl on urethane can be detected at the peak of 3301 cm^{-1} and in the wavenumber at range 3326–3428 cm^{-1}. This has also been studied and detected by Mutsuhisa et al. [45] and Lampman et. al. [46]. In this research, the proton acceptor is carbonyl (-C=O) while the proton donor is an amine (-NH) to form a hydrogen bond. The MDI chemical structure has the electrostatic capability that produces dipoles from several atoms such as hydrogen, oxygen, and nitrogen atoms. The characteristic of isocyanates causing them are highly reactive [47].

MDI was one of the isocyanates used in this study, has an aromatic group, and is more reactive compared to aliphatic group isocyanates such as hexamethylene diisocyanate (HDI) or isophorone diisocyanate (IPDI). Isocyanates have two groups of isocyanates on each molecule. Diphenylmethane diisocyanate is an exception owing to its structure consisting of two, three, four, or more isocyanate groups [48]. The use of PEG 400 in this study as a chain extender for polyurethane increases the chain mobility of polyurethane at an optimal amount. The properties of polyurethane are contributed by hard and soft copolymer segments of both polyol monomers and MDI. This makes the hard segment of urethane serves as a crosslinking site between the soft segments of the polyol [47].

The mechanism of the prepolymerization in urethane chains formation is a nucleophilic substitution reaction as studied by Yong et al. [49]. However, this study found amines as nucleophiles. Amine attacks carbonyl on isocyanate in MDI in order to form two resonance structures of intermediate complexes A and B (Figure 4). Intermediate complex B has a greater tendency to react with polyols due to stronger carbonyl (C=O) bonds than C=N bonds on intermediate complexes A. Thus, intermediate complex B is more stable than intermediate complex A, as suggested by previous researchers conducted by Wong and Badri [41].

Moreover, oxygen is more electronegative than nitrogen causing cations (H+) to tend to attack -CN bonds compared to -CO. The combination between long polymer chain and low crosslinking content gives the polymer elastic properties whereas short-chain and high crosslinking produce hard and rigid polymers. Crosslinking in polymers consists of three-dimensional networks with high molecular weight. In some aspects, polyurethane can be a macromolecule, a giant molecule [50].

However, complexes A and B intermediate were produced after the nucleophile of PEG attacking the isocyanate group in the MDI. However, PEG contains oxygen atoms that are more electronegative than nitrogen atoms inside the PKO-p chemical structure causing the reaction of nucleophilic substitution that occurs in PKO-p. Furthermore, amine has a higher probability of reacting compared to hydroxyl [51]. Amine with high alkalinity reacts with carbon atoms on MDI as proposed by Wong and Badri [41].

The production of intermediate complexes unstabilizes the alkyl ions; nevertheless, the long carbon chains of PKO-p ensure the stability of alkyl ions. The addition of PEG in this study is imperative, not merely to increase the chain length of PU but also to avoid the production of urea as a byproduct after the NCO group reacts with H_2O from the environment. If the NCO group reacts with the excess water in the environment, the formation of urea and carbon dioxide gas will also occur excessively (Figure 5). This reaction can cause a polyurethane foam, not polyurethane film as we studied the film.

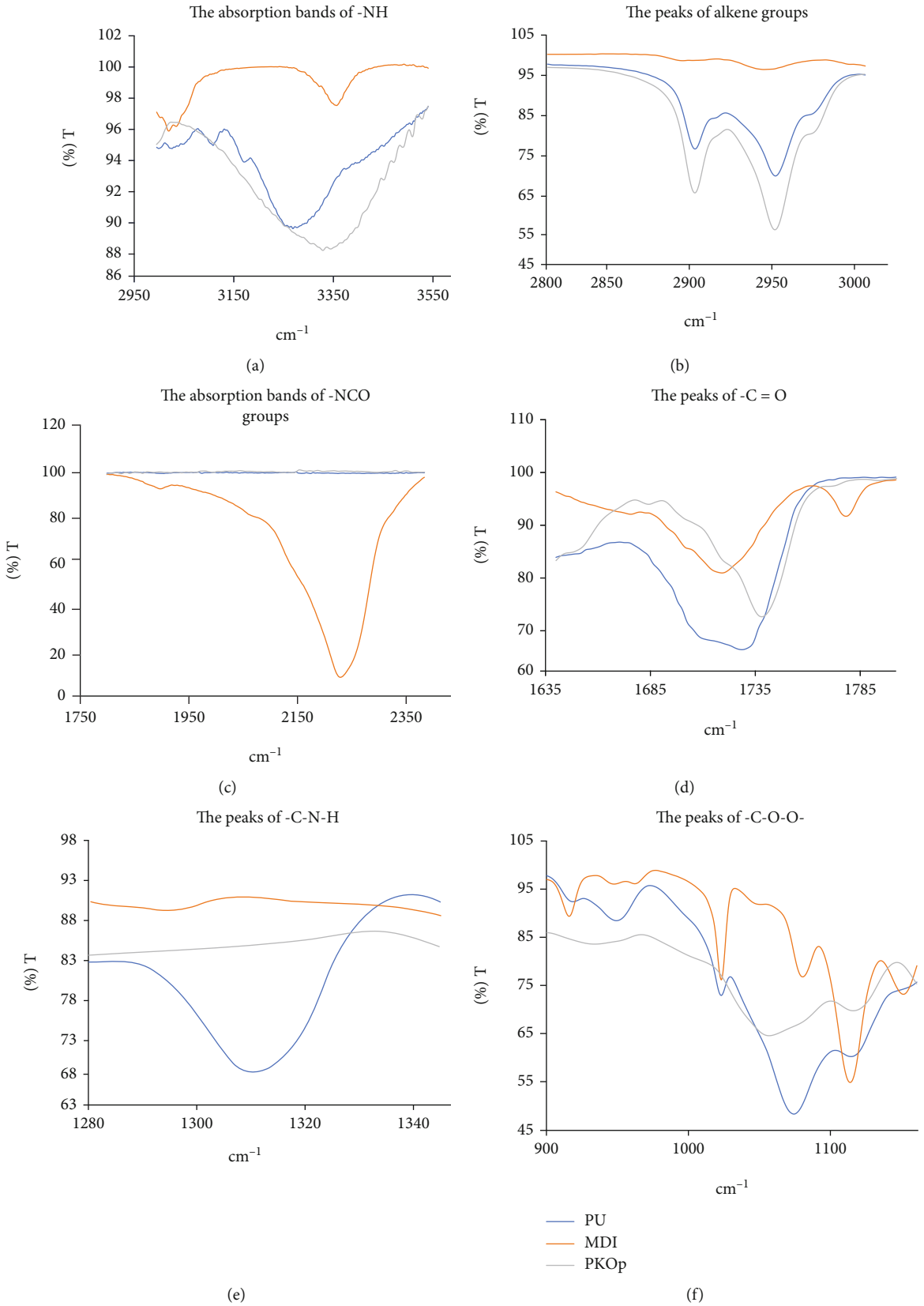

Figure 3: FTIR spectra of several important peaks between polyurethane, PKO-p, and MDI.

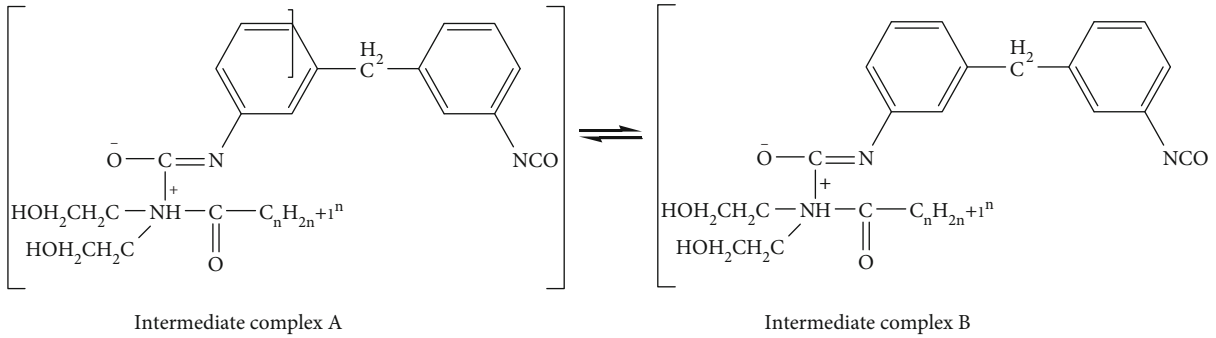

Figure 4: The formation of intermediate complexes.

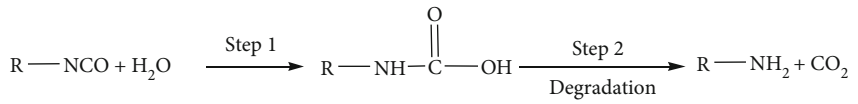

Figure 5: The reaction between the NCO group and water producing carbon dioxide.

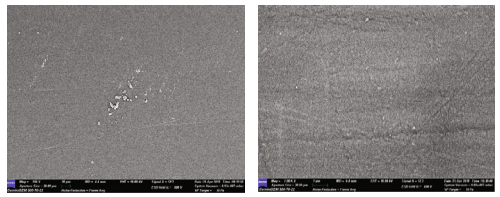

Figure 6: The micrograph of polyurethane films was analyzed by FESEM at (a) 200x and (b) 5000x magnifications.

Furthermore, the application of PEG can influence the conductivity of PU whereby Porcarelli et al. [52] have reported the application of PEG using several molecular weights. PEG 1500 decreased the conductivity of PU in consequence of the semicrystalline phase of PEG 1500 that acted as a poor ion-conducting phase for PU. It is also well known that PEG with a molecular weight of more than 1000 g•mol^{-1} tends to crystallize with deleterious effects on room temperature ionic conductivity [52].

3.2. Morphological Analysis. The field emission scanning electron microscope micrograph in Figure 6 shows the formation of a uniform polymer film contributed by the polymerization method applied. The magnification used for this surface analysis ranged from 200 to 5000x. The polymerization method can also avoid the failure of the reaction in PU polymerization. Furthermore, no trace of separation was detected by FESEM. This has also been justified by the wavelengths obtained by the FTIR spectra above.

3.3. The Crosslinking Analysis. Soxhlet analysis was applied to determine the degree of crosslinking between the hard segments and the soft segments in the polyurethane. The urethane group on the hard segment along the polyurethane chain is polar [53]. Therefore, during the testing, it was very difficult to dissolve in toluene, as the testing reagent. The degree of crosslinking is determined by the percentage of the gel content. The analysis result obtained from the soxhlet testing indicated a 99.3% gel content. This is significant in getting a stable polymer at a higher working temperature [54, 55].

$$\text{Gel content}(\%) = \frac{(0.6 - 0.301)\,\text{g}}{0.301\text{g}} \times 100\% = 99.33\%. \quad (2)$$

3.4. The Thermal Analysis. Thermogravimetric analysis can be used to observe the material mass based on temperature shift. It can also examine and estimate the thermal stability and materials properties such as the alteration weight owing to absorption or desorption, decomposition, reduction, and oxidation. The material composition of polymer is specified by analyzing the temperatures and the heights of the individual mass steps [56]. Figure 7 shows the TGA and derivative thermogravimetry (DTG) thermograms of polyurethane. The percentage weight loss (%) is listed in Table 2. Generally, only a small amount of weight was observed. It is shown in Figure 7 in the region of 45–180°C. This is due to the presence of condensation on moisture and solvent residues.

$T_{\max}$: the temperature of polyurethane started to degrade; T_{d1}: thermal degradation first; T_{d2}: thermal degradation second; T_{d3}: thermal degradation third.

The bio-based polyurethane is thermally stable up to 240°C before it has undergone thermal degradation [57]. The first stage of thermal degradation (T_{d1}) on polyurethane films was shown in the region of 200–290°C as shown in Figure 7. The T_{d1} is associated with degradation of the hard segments of the urethane bond, forming alcohol or degradation of the polyol chains and releasing of isocyanates [58], primary and secondary amines, as well as carbon dioxide [59, 60]. Meanwhile, the second thermal degradation stage (T_{d2}) of polyurethane films experienced a weight loss of 39.29%. This endotherm of T_{d2} is related to the dimerization of isocyanates to form carbodiimides and release CO_2. The formed carbodiimide reacts with alcohol to form urea. The

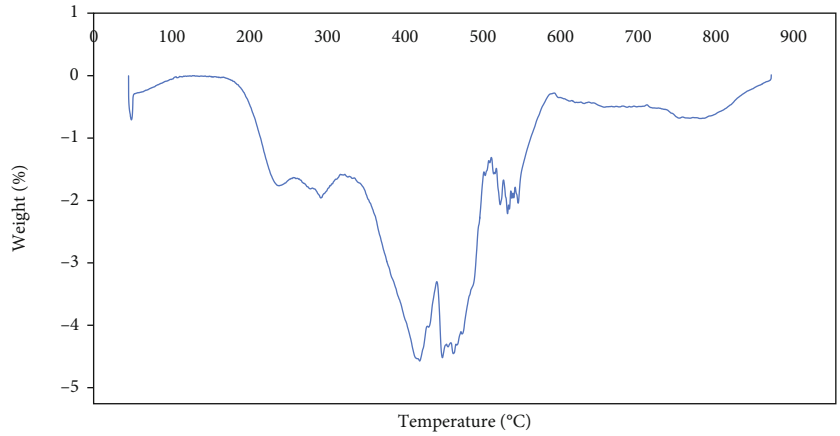

Figure 7: DTG thermogram of polyurethane film.

Table 2: Weight loss percentage (wt%) and thermal degradation (Td) of polyurethane film.

	% weight loss (*wt*%) and thermal degradation (T_d)			Total of weight loss (%)	Residue after 550°C (%)
T_{max}, (°C)	T_{d1}, 200–290°C	T_{d2}, 350–500°C	T_{d3}, 500–550°C		
240	8.04	39.29	34.37	81.7	18.3

third stage of thermal degradation (T_{d3}) is related to the degradation of urea [58] and the soft segment on polyurethane.

Generally, DSC analysis exhibited thermal transitions as well as the initial crystallization and melting temperatures of the polyurethane [61]. It serves to analyze changes in thermal behavior due to changes occurring in the chemical chain structure based on the T_g of the sample obtained from the DSC thermogram (Figure 8). DSC analysis on polyurethane film was performed in the temperature at the range 100°C to 200°C of using nitrogen gas as a blanket as proposed by Furtwengler et al. [62]. The glass transition temperature on polyurethane was above room temperature, at 78.1°C indicated the state of glass on polyurethane. The presence of MDI contributes to the formation of hard segments in polyurethanes. Porcarelli et al. [52] stated that possessing a low T_g may contribute to PU conductivity.

During polymerization, this hard segment restricts the mobility of the polymer chain [63] owing to the steric effect on the benzene ring in the hard segment. The endothermic peak of acetone used as the solvent in this study was supposedly at 56°C. However, the acetone peak was not detected in the DSC and TGA instruments, which can be concluded the acetone was completely evaporated during the polyurethane synthesis. The presence of acetone in the synthesis was to lower the reaction kinetics.

3.5. The Solubility and Mechanical Properties of the Polyurethane Film. The chemical resistivity of a polymer will be the determinant in performing as a conductor. Thus, its solubility in various solvents was determined by dissolving the polymer in selected solvents such as hexane, benzene, acetone, THF, DMF, and DMSO. On the other hand, the mechanical properties of polyurethane were determined based on the standard testing following ASTM D638. The results from the polyurethane film solubility and tensile test are shown in Table 3. Polyurethane films were insoluble with acetone, hexane, and benzene and are only slightly soluble in THF, DMF, and DMSO solutions. While the tensile strength of a PU film indicated how much elongation load the film was capable of withstanding the material before breaking.

The tensile stress, strain, and modulus of polyurethane film also indicated that polyurethane has good mechanical properties that are capable of being a supporting substrate for the next stage of the study. In the production of polyurethane, the properties of polyurethane are easily influenced by the content of MDI and polyol used. The length of the chain and its flexibility are contributed by the polyol which makes it elastic. High crosslinking content can also produce hard and rigid polymers. MDI is a major component in the formation of hard segments in polyurethane. It is this hard segment that determines the rigidity of the PU. Therefore, high isocyanate content results in higher rigidity on PU (Petrovic et al. 2002). Thus, the polymer has a higher resistance to deformation and more stress can be applied to the PU.

3.6. The Conductivity of the Polyurethane as a Polymeric Film on SPE. Polyurethane film was deposited onto the screen-printed electrode by casting method as shown in Figure 1. After that, the modified electrode was analyzed using cyclic voltammetry and differential pulse voltammetry in order to study the behavior of the modified electrode. The modified electrode was tested in a 0.1 mmol·L^{-1} KCl solution containing 5 mmol·L^{-1} ($K_3Fe(CN)_6$). The use of potassium ferricyanide is intended to increase the sensitivity of the KCl solution. The conductivity of the modified electrode was studied. The electrode was analyzed by cyclic voltammetry method with a potential range of -1.00 to +1.00 with a scan rate of 0.05 V·s^{-1}. The voltammograms at the electrode have shown a specific redox reaction. Furthermore, the conductivity of the modified electrode is lower due to the use of polyurethane. This occurs due to PU being a natural polymer produced from the polyol of palm kernel oil-based

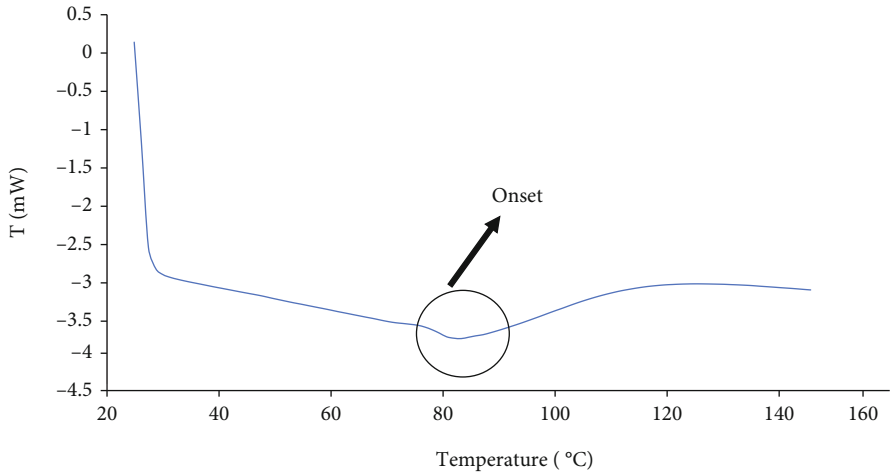

Figure 8: DSC thermogram of polyurethane film.

Table 3: The solubility and mechanical properties of the polyurethane film.

Parameters		Polyurethane film
Solubility	Benzene	Insoluble
	Hexane	Insoluble
	Acetone	Insoluble
	THF	Less soluble
	DMF	Less soluble
	DMSO	Less soluble
Stress (MPa)		8.53
Elongation percentage (%)		43.34
Strain modulus (100) (MPa)		222.10

polyol. The electrochemical signal at the electrode is low if there is a decrease in electrochemical conductivity [64]. It can be concluded that polyurethane is a biopolymer with a low current value. The current of the modified electrode was found at 5.3×10^{-5} A or 53 μA. Nevertheless, the current of PU in this study showed better results compared to Bahrami et al. (2019) that reported the current of PU as 1.26×10^{-6} A, whereas Li et al. [65] reported the PU current in their study was even very low, namely, 10^{-14} A. The PU can obtain a current owing to the benzene ring in the hard segment (MDI) could exhibit the current by inducing electron delocalization along the polyurethane chain [66]. The PU can also release a current caused by PEG. The application of PEG as polyol has been studied by Porcarelli et al. [52] that reported that the current of PU based on PEG–polyol was 9.2×10^{-8} A.

According to Figure 9, it can be concluded that the anodic peak present in the modified electrode was at +0.5 V, and it also represented the anodic peak of the SPE-PU. The first oxidation signal on both electrodes ranged from -0.2 to +1.0 V, which revealed a particular oxidative peak at a potential of +0.5 V.

Figure 10 also presents the DPV voltammogram of the modified electrode. DPV is a measurement based on the difference in potential pulses that produce an electric current. Scanning the capability pulses to the working electrode will produce different currents. Optimal peak currents will be produced to the reduction capacity of the redox material. The peak current produced is proportional to the concentration of the redox substance and can be detected up to a concentration below 10^{-8} M. DPV was conducted to obtain the current value that is more accurate than CV [67].

This study used a redox pair ($K_3Fe(CN)_6$) as a test device (probe). The currents generated by SPE-PU and proved by CV and DPV have shown conductivity on polyurethane films. This suggests that polyurethane films can conduct electron transfer. The electrochemical area on the modified electrode can be calculated using the formula from Randles-Sevcik [68], where the electrochemical area for SPE-PU is considered to be A, using Equation (3):

$$Current \text{ of } SPE - PU, Ip = 2.65 \times 105\, ACn^{3/2}v^{1/2}D^{1/2}, \quad (3)$$

where $n - 1$ is the amount of electron transfer involved, while C is the solvent concentration used (mmol·L^{-1}) and the value of D is the diffusion constant of 5 mmol·L^{-1} at ($K_3Fe(CN)_6$) dissolved using 0.1 mmol·L^{-1} KCl. The estimated surface area of the electrode (Figure 1) was 0.2 cm^2, where the length and width of the electrode used during the study was 0.44 cm × 0.44 cm, while the surface area of the SPE-PU was 0.25 cm^2 with the length and width of the electrode estimated at 0.5 cm × 0.5 cm, causing the SPE-PU has a larger surface. The corresponding surface concentration (τ) (mol/cm^2) is measured using Equation (4).

$$Ip = \left(\frac{n2F2}{4RT}\right) A\tau v, \quad (4)$$

where I_p is the peak current (A), while A is the surface area of the electrode (cm^2), the value of v is the applied scan rate (mV/s) and F is the Faraday constant (96,584 C/mol), R is the constant ideal gas (8.314 J/mol K), and T is the temperature used during the experiment being conducted (298 K)

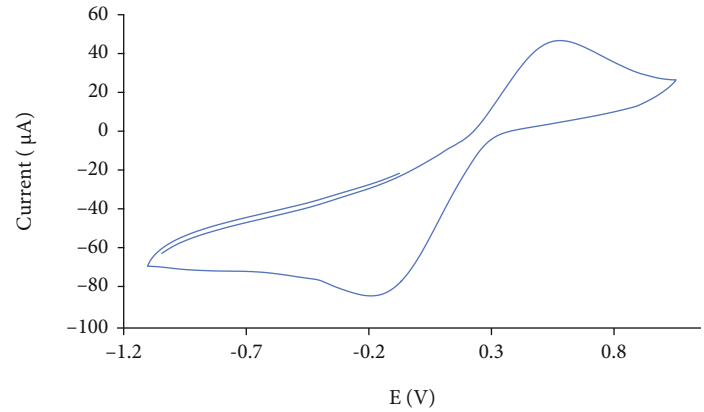

Figure 9: The voltammogram of SPE-PU modified electrode after analyzed using cyclic voltammetry technique.

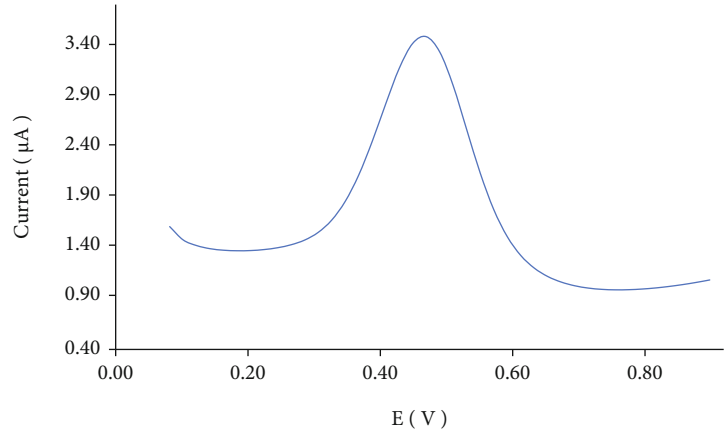

Figure 10: The voltammogram of SPE–PU modified electrode after analyzed using differential pulse voltammetry technique.

[69]. The application of PKO-p to produce a conducting polymer will be a great prospect as this material can be employed in the analytical industry in order to modify electrodes for electrochemical purposes.

Furthermore, a number of palm oils are abundant in Malaysia and Indonesia such as palm stearin and refined-bleached-deodorized (RBD) palm oil. They have several benefits such as being sustainable, cheap, and environmentally biodegradable. These palms are the potential to produce biomaterials that can be used to replace other polymers that are chemical based [17]. Several studies have been reported the application of PU to produce elastic conductive fibres and films owing to it being highly elastic, scratch-resistant, and adhesive [70]; thus, it is easy for PU to adhere to the screen-printed electrode to modify the electrode. PU is also being used as a composite material to make elastic conducting composite films [71].

4. Conclusion

Polyurethane film was prepared by prepolymerization between palm kernel oil-based polyol (PKO-p) with MDI. The presence of PEG 400 as the chain extender formed free-standing flexible film. Acetone was used as the solvent to lower the reaction kinetics since the prepolymerization was carried out at room temperature. The formation of urethane links (-NHC(O) backbone) after polymerization was confirmed by the absence of absorption bands at 2241 cm^{-1} associated with the N=C=O bond stretching and the presence of N-H peak at 3300 cm^{-1}, carbonyl (C=O) at 1710 cm^{-1}, carbamate (C-N) at 1600 cm^{-1}, ether (C-O-C) at 1065 cm^{-1}, benzene ring (C=C) at 1535 cm^{-1} in the bio-based polyurethane chain structure. Soxhlet analysis for the determination of crosslinking on polyurethane films has yielded a high percentage of 99.33%. This is contributed by the hard segments formed from the reaction between isocyanates and hydroxyl groups causing elongation of polymer chains. FESEM analysis exhibited an absence of phase separation and smooth surface. Meanwhile, the current of the modified electrode was found at 5.2×10^{-5} A. This bio-based polyurethane film can be used as a conducting biopolymer, and it is very useful for other studies such as electrochemical sensor purposes. Furthermore, advanced technologies are promising, and the future of bio-based polyol looks very bright.

Data Availability

All data experiments can be found in the manuscript.

Conflicts of Interest

The authors declare no conflict of interest.

Acknowledgments

The authors would like to thank Alma Ata University for the sponsorship given to the first author. We would like to also thank the Department of Chemical Sciences, Universiti Kebangsaan, Malaysia, for the laboratory facilities and CRIM, UKM, for the analysis infrastructure.

References

[1] S. A. Alqarni, M. A. Hussein, A. A. Ganash, and A. Khan, "Composite material–based conducting polymers for electrochemical sensor applications: a mini review," *BioNanoScience.*, vol. 10, no. 1, pp. 351–364, 2020.

[2] M. Z. Dzulkipli, J. Karim, A. Ahmad et al., "The influences of 1-butyl-3-methylimidazolium tetrafluoroborate on electrochemical, thermal and structural studies as ionic liquid gel polymer electrolyte," *Polymers*, vol. 13, no. 8, pp. 1277–1294, 2021.

[3] P. Sengodu and A. D. Deshmukh, "Conducting polymers and their inorganic composites for advanced Li-ion batteries: a review," *RSC Advances*, vol. 5, no. 52, pp. 42109–42130, 2015.

[4] B. Wang, L. Wang, X. Li et al., "Template-free fabrication of vertically-aligned polymer nanowire array on the flat-end tip for quantifying the single living cancer cells and nanosurface interaction," *Manufacturing Letters*, vol. 16, pp. 27–31, 2018.

[5] S. Ghosh, S. Ganguly, S. Remanan et al., "Ultra-light weight, water durable and flexible highly electrical conductive polyurethane foam for superior electromagnetic interference shielding materials," *Journal of Materials Science: Materials in Electronics*, vol. 29, no. 12, pp. 10177–10189, 2018.

[6] T. Pan and Q. Yu, "comprehensive evaluation of anti-corrosion capacity of electroactive polyaniline for steels," *Anti-Corrosion Methods and Materials*, vol. 63, no. 5, pp. 360–368, 2016.

[7] M. Ladan, W. J. Basirun, S. N. Kazi, and F. A. Rahman, "Corrosion protection of AISI 1018 steel using co-doped TiO_2/polypyrrole nanocomposites in 3.5% NaCl solution," *Materials Chemistry and Physics*, vol. 192, pp. 361–373, 2017.

[8] T. Fei, Y. Li, B. Liu, and C. Xia, "Flexible polyurethane/boron nitride composites with enhanced thermal conductivity," *High Performance Polymers*, vol. 32, no. 3, pp. 1–10, 2020.

[9] S. Guo, C. Zhang, M. Yang et al., "A facile and sensitive electrochemical sensor for non-enzymatic glucose detection based on three-dimensional flexible polyurethane sponge decorated with nickel hydroxide," *Analytica Chimica Acta*, vol. 1109, pp. 130–139, 2020.

[10] V. H. Tran, J. D. Kim, J. H. Kim, S. K. Kim, and J. M. Lee, "Influence of cellulose nanocrystal on the cryogenic mechanical behavior and thermal conductivity of polyurethane composite," *Journal of Polymers and The Environment*, vol. 28, no. 4, pp. 1169–1179, 2020.

[11] I. R. Vieira, L. D. Costa, G. D. Miranda et al., "Waterborne poly (urethane – urea)s nanocomposites reinforced with clay, reduced graphene oxide and respective hybrids: synthesis, stability and structural characterization," *Journal of Polymers and the Environment*, vol. 28, no. 1, pp. 74–90, 2020.

[12] K. H. Badri, "Biobased polyurethane from palm kernel oil-based polyol," in *Polyurethane*, F. Zafar and E. Sharmin, Eds., pp. 447–470, InTechOpen, Rijeka, Croatia, 2012.

[13] M. Borowicz, J. P. Sadowska, J. Lubczak, and B. Czuprynski, "Biodegradable, flame–retardant, and bio-based rigid polyurethane/polyisocyanurate foams for thermal insulation application," *Polymers*, vol. 11, no. 11, pp. 1816–1839, 2019.

[14] M. A. Mohd Noor, T. N. M. Tuan Ismail, and R. Ghazali, "Bio-based content of oligomers derived from palm oil: sample combustion and liquid scintillation counting technique," *Malaysia Journal of Analytical Science*, vol. 24, pp. 906–917, 2020.

[15] R. Mustapha, A. R. Rahmat, R. Abdul Majid, and S. N. H. Mustapha, "Vegetable oil-based epoxy resins and their composites with bio-based hardener: a short review," *Polymer- Plastic Technology and Materials*, vol. 58, no. 12, pp. 1311–1326, 2019.

[16] A. A. Septevani, D. A. C. Evans, C. Chaleat, D. J. Martin, and P. K. Annamalai, "A systematic study substituting polyether polyol with palm kernel oil based polyester polyol in rigid polyurethane foam," *Industrial Crops and Products*, vol. 66, pp. 16–26, 2015.

[17] R. Tajau, R. Rohani, M. S. Alias et al., "Emergence of polymeric material utilising sustainable radiation curable palm oil-based products for advanced technology applications," *Polymers*, vol. 13, no. 11, pp. 1865–1886, 2021.

[18] S. S. Priya, M. Karthika, S. Selvasekarapandian, and R. Manjuladevi, "Preparation and characterization of polymer electrolyte based on biopolymer I-carrageenan with magnesium nitrate," *Solid State Ionics*, vol. 327, pp. 136–149, 2018.

[19] T. Romaskevic, S. Budriene, K. Pielichowski, and J. Pielichowski, "Application of polyurethane-based materials for immobilization of enzymes and cells: a review," *Chemija*, vol. 17, pp. 74–89, 2006.

[20] K. M. Zia, S. Anjum, M. Zuber, M. Mujahid, and T. Jamil, "Synthesis and molecular characterization of chitosan based polyurethane elastomers using aromatic diisocyanate," *International Journal of Biological Macromolecules*, vol. 66, pp. 26–32, 2014.

[21] A. Badan and T. M. Majka, "The influence of vegetable – oil based polyols on physico – mechanical and thermal properties of polyurethane foams," in *Proceedings of the 21st International Electronic Conference on Synthetic Organic Chemistry, Santiago de Compostela*, pp. 1–7, Spain, 2017.

[22] M. A. Munir, L. Y. Heng, E. E. Sage, M. M. M. Mackeen, and K. H. Badri, "Histamine detection in mackerel (Scomberomorus Sp.) and its products derivatized with 9-flourenilmethylchloroformate," *Chemistry*, vol. 22, no. 2, pp. 243–251, 2021.

[23] M. A. Munir, L. Y. Heng, and K. H. Badri, "Polyurethane modified screen-printed electrode for the electrochemical detection of histamine in fish," *IOP Conference Series: Earth and Environmental Science*, vol. 880, no. 1, article 012032, 2021.

[24] M. A. Munir, M. M. M. Mackeen, L. Y. Heng, and K. H. Badri, "Study of histamine detection using liquid chromatography and gas chromatography," *ASM Science Journal*, vol. 16, pp. 1–9, 2021.

[25] J. O. Akindoyo, M. D. H. Beg, S. Ghazali, M. R. Islam, N. Jeyaratnam, and A. R. Yuvaraj, "Polyurethane types, synthesis, and applications – a review," *RSC Advances*, vol. 6, no. 115, pp. 114453–114482, 2016.

[26] P. Janpoung, P. Pattanauwat, and P. Potiyaraj, "Improvement of electrical conductivity of polyurethane/polypyrrole blends

by graphene," *Key Engineering Materials*, vol. 831, pp. 122–126, 2020.

[27] M. S. Su'ait, A. Ahmad, K. H. Badri et al., "The potential of polyurethane bio-based solid polymer electrolyte for photo-electrochemical cell application," *International Journal of Hydrogen Energy*, vol. 39, no. 6, pp. 3005–3017, 2014.

[28] M. Kotal, S. K. Srivastava, and B. Paramanik, "Enhancements in conductivity and thermal stabilities of polypyrrole/polyurethane nanoblends," *The Journal of Physical Chemistry C*, vol. 115, no. 5, pp. 1496–1505, 2011.

[29] J. Wang, L. Xiao, X. Du, J. Wang, and H. Ma, "Polypyrrole composites with carbon materials for supercapacitors," *Chemical Papers*, vol. 71, no. 2, pp. 293–316, 2017.

[30] E. Harmayani, V. Aprilia, and Y. Marsono, "Characterization of glucomannan from _Amorphophallus oncophyllus_ and its prebiotic activity _in vivo_," *Carbohydrate Polymers*, vol. 112, pp. 475–479, 2014.

[31] A. Inayatullah, H. A. Badrul, and M. A. Munir, "Fish analysis containing biogenic amines using gas chromatography flame ionization detector," *Science and Technology Indonesia*, vol. 6, no. 1, pp. 1–7, 2021.

[32] J. C. Kilele, R. Chokkareddy, N. Rono, and G. G. Redhi, "A novel electrochemical sensor for selective determination of theophylline in pharmaceutical formulations," *Journal of the Taiwan Institute of Chemical Engineers*, vol. 111, pp. 228–238, 2020.

[33] E. Nurwanti, M. Uddin, J. S. Chang et al., "Roles of sedentary behaviors and unhealthy foods in increasing the obesity risk in adult men and women: a cross-sectional national study," *Nutrients*, vol. 10, no. 6, pp. 704–715, 2018.

[34] R. Chokkareddy, S. Kanchi, and Inamuddin, "Simultaneous detection of ethambutol and pyrazinamide with IL@Co-Fe_2O_4NPs@MWCNTs fabricated glassy carbon electrode," *Scientific Reports*, vol. 10, no. 1, article 13563, 2020.

[35] J. C. Kilele, R. Chokkareddy, and G. G. Redhi, "Ultra-sensitive electrochemical sensor for fenitrothion pesticide residues in fruit samples using $_2O_4$ nanocomposite," *Microchemical Journal*, vol. 164, article 106012, 2021.

[36] H. Degefu, M. Amare, M. Tessema, and S. Admassie, "Lignin modified glassy carbon electrode for the electrochemical determination of histamine in human urine and wine samples," *Electrochimica Acta*, vol. 121, pp. 307–314, 2014.

[37] M. A. Munir, K. H. Badri, L. Y. Heng et al., "The application of polyurethane-LiClO4to modify screen-printed electrodes analyzing histamine in mackerel using a voltammetric approach," *ACS Omega*, vol. 7, no. 7, pp. 5982–5991, 2022.

[38] P. Nakthong, T. Kondo, O. Chailapakul, and W. Siangproh, "Development of an unmodified screen-printed graphene electrode for nonenzymatic histamine detection," *Analytical Methods*, vol. 12, no. 44, pp. 5407–5414, 2020.

[39] N. Baig, M. Sajid, and T. A. Saleh, "Recent trends in nanomaterial-modified electrodes for electroanalytical applications," *Trends in Analytical Chemistry*, vol. 111, pp. 47–61, 2019.

[40] K. H. Badri, S. H. Ahmad, and S. Zakaria, "Production of a high-functionality RBD palm kernel oil-based polyester polyol," *Journal of Applied Polymer Science*, vol. 81, no. 2, pp. 384–389, 2001.

[41] C. S. Wong and K. H. Badri, "Chemical analyses of palm kernel oil-based polyurethane prepolymer," *Materials Sciences and Applications*, vol. 3, no. 2, pp. 78–86, 2012.

[42] H. A. Hamuzan and K. H. Badri, "The role of isocyanates in determining the viscoelastic properties of polyurethane," *AIP Conference Proceedings*, vol. 1784, no. 1, article 030019, 2016.

[43] K. Mishra, R. Narayan, K. V. S. N. Raju, and T. M. Aminabhavi, "Hyperbranched polyurethane (HBPU)-urea and HBPU-imide coatings: effect of chain extender and NCO/OH ratio on their properties," *Progress in Organic Coatings*, vol. 74, no. 1, pp. 134–141, 2012.

[44] I. Clemitson, *Castable Polyurethane Elastomers*, Taylor & Francis Group, New York, 2008.

[45] F. Mutsuhisa, K. Ken, and N. Shohei, "Microphase separated structure and mechanical properties of norbornane diisocyanate–based polyurethane," *Polymer*, vol. 48, no. 4, pp. 997–1004, 2007.

[46] G. M. Lampman, D. L. Pavia, G. S. Kriz, and J. R. Vyvyan, *Spectroscopy*, Brooks/Cole Cengage Learning, Belmont, USA, 4th Edition edition, 2010.

[47] A. Leykin, L. Shapovalov, and O. Figovsky, "Non – isocyanate polyurethanes – yesterday, today and tomorrow," *Alternative Energy and Ecology*, vol. 191, no. 3–4, pp. 95–108, 2016.

[48] B. Nohra, L. Candy, J. F. Blancos, C. Guerin, Y. Raoul, and Z. Mouloungui, "From petrochemical polyurethanes to bio-based polyhydroxyurethanes," *Macromolecules*, vol. 46, no. 10, pp. 3771–3792, 2013.

[49] Z. Yong, Z. M. Bo, W. Bo, J. Z. Lin, and N. Jun, "Synthesis and properties of novel polyurethane acrylate containing 3-(2-hydroxyethyl) isocyanurate segment," *Progress in Organic Coatings*, vol. 67, pp. 264–268, 2009.

[50] Z. S. Petrovic, "Polyurethanes from vegetable oils," *Polymer Reviews*, vol. 48, no. 1, pp. 109–155, 2008.

[51] R. Herrington and K. Hock, *Flexible Polyurethane Foams*, Dow Chemical Company, Midlan, 2nd Edition edition, 1997.

[52] L. Porcarelli, K. Manojkumar, H. Sardon et al., "Single ion conducting polymer electrolytes based on versatile polyurethanes," *Electrochimica Acta*, vol. 241, pp. 526–534, 2017.

[53] L. Cuve, J. P. Pascault, G. Boiteux, and G. Seytre, "Synthesis and properties of polyurethanes based on polyolefine: 1. Rigid polyurethanes and amorphous segmented polyurethanes prepared in polar solvents under homogeneous conditions," *Polymer*, vol. 32, no. 2, pp. 343–352, 1991.

[54] S. K. Rogulska, A. Kultys, and W. Podkoscielny, "Studies on thermoplastic polyurethanes based on new diphenylethane-derivative diols. II. Synthesis and characterization of segmented polyurethanes from HDI and MDI," *European Polymer Journal*, vol. 43, no. 4, pp. 1402–1414, 2007.

[55] S. Ibrahim, K. Badri, C. T. Ratnam, N. H. M. Ali, and M. A. Munir, "Radiation dose required for the vulcanization of natural rubber latex via hybrid gamma radiation and peroxide vulcanizations," *IOP Conference Series: Materials Science and Engineering*, vol. 555, 2019.

[56] M. Y. Alamawi, F. H. Khairuddin, N. I. M. Yusoff, K. Badri, and H. Ceylan, "Investigation on physical, thermal and chemical properties of palm kernel oil polyol bio-based binder as a replacement for bituminous binder," *Construction and Building Materials*, vol. 204, pp. 122–131, 2019.

[57] A. Agrawal, R. Kaur, and R. S. Walia, "PU foam derived from renewable sources: perspective on properties enhancement: an overview," *European Polymer Journal*, vol. 95, pp. 255–274, 2017.

[58] M. Berta, C. Lindsay, G. Pans, and G. Camino, "Effect of chemical structure on combustion and thermal behaviour of

polyurethane elastomer layered silicate nanocomposites," *Polymer Degradation and Stability*, vol. 91, no. 5, pp. 1179–1191, 2006.

[59] M. A. Corcuera, L. Rueda, A. Saralegui et al., "Effect of diisocyanate structure on the properties and microstructure of polyurethanes based on polyols derived from renewable resources," *Journal of Applied Polymer Science*, vol. 122, no. 6, pp. 3677–3685, 2011.

[60] X. Pan and D. C. Webster, "New biobased high functionality polyols and their use in polyurethane coatings," *ChemSusChem*, vol. 5, no. 2, pp. 419–429, 2012.

[61] F. H. Khairuddin, N. I. M. Yusof, K. Badri, H. Ceylan, and S. N. M. Tawil, "Thermal, chemical and imaging analysis of polyurethane/cecabase modified bitumen," *IOP Conference Series: Materials Science and Engineering*, vol. 512, article 012032, 2018.

[62] P. Furtwengler, R. Perrin, A. Redl, and L. Averous, "Synthesis and characterization of polyurethane foams derived of fully renewable polyester polyols from sorbitol," *European Polymer Journal*, vol. 97, pp. 319–327, 2017.

[63] D. Ren and C. E. Frazier, "Structure-property behavior of moisture-cure polyurethane wood adhesives: influence of hard segment content," *Adhesion and Adhesives*, vol. 45, pp. 118–124, 2013.

[64] H. A. El-Raheem, R. Y. A. Hassan, R. Khaled, A. Farghali, and I. M. El-Sherbiny, "Polyurethane-doped platinum nanoparticles modified carbon paste electrode for the sensitive and selective voltammetric determination of free copper ions in biological samples," *Microchemical Journal*, vol. 155, article 104765, 2020.

[65] H. Li, D. Yuan, P. Li, and C. He, "High conductive and mechanical robust carbon nanotubes/waterborne polyurethane composite films for efficient electromagnetic interference shielding," *Composites Part A Applied Science and Manufacturing*, vol. 121, pp. 411–417, 2019.

[66] C. S. Wong, K. H. Badri, N. Ataollahi, K. P. Law, M. S. Su'ait, and N. I. Hassan, "Synthesis of new bio–based solid polymer electrolyte polyurethane – $LiClO_4$ via prepolymerization method: effect of NCO/OH ratio on their chemical, thermal properties and ionic conductivity," *World Academy of Science, Engineering and Technology, International Journal of Chemical, Molecular, Nuclear, Materials and Metallurgical Engineering*, vol. 8, pp. 1243–1250, 2014.

[67] K. J. Lee, N. Elgrishi, B. Kandemir, and J. L. Dempsey, "Electrochemical and spectroscopic methods for evaluating molecular electrocatalysts," *Nature Reviews Chemistry*, vol. 1, no. 5, pp. 1–14, 2018.

[68] N. Butwong, J. Khajonklin, A. Thongbor, and J. H. T. Luong, "Electrochemical sensing of histamine using a glassy carbon electrode modified with multiwalled carbon nanotubes decorated with Ag-Ag_2O nanoparticles," *Microchimica Acta*, vol. 186, no. 11, article 714, 2019.

[69] D. Koita, T. Tzedakis, C. Kane, M. Diaw, O. Sock, and P. Lavedan, "Study of the histamine electrochemical oxidation catalyzed by nickel sulfate," *Electroanalysis*, vol. 26, no. 10, pp. 2224–2236, 2014.

[70] M. G. Tadesse, D. A. Mengistie, Y. Chen, L. Wang, C. Loghin, and V. Nierstrasz, "Electrically conductive highly elastic polyamide/lycra fabric treated with PEDOT: PSS and polyurethane," *Journal of Materials Science*, vol. 54, no. 13, pp. 9591–9602, 2019.

[71] H. Khatoon and S. Ahmad, "A review on conducting polymer reinforced polyurethane composites," *Journal of Industrial and Engineering Chemistry*, vol. 53, pp. 1–22, 2017.